Patagonian and southern South Atlantic view of Holocene climate

Kaplan, M.R.[1], Schaefer, J.M.[1,2], Strelin, J.A.[3], Denton, G.H.[4], Anderson, R.F.[1,2], Vandergoes, M.J.[5], Finkel, R.C.[6], Schwartz, R.[1], Travis, S.G.[7], Garcia, J.L.[4,8], Martini, M.[3], Nielsen, S.[9]

[1] *Geochemistry, Lamont-Doherty Earth Observatory, Palisades, NY 10964, USA*
[2] *Department of Earth and Environmental Sciences, Columbia University, New York, NY 10027, USA*
[3] *Centro de Investigaciones en Ciencias de la Tierra (CONICET-UNC), Córdoba, Argentina*
[4] *Dept. of Earth Sciences and Climate Change Institute, University of Maine, Orono, ME 04469, USA*
[5] *GNS Science, Lower Hutt 5010 New Zealand*
[6] *Dept. of Earth and Planetary Sciences, University of California, Berkeley, CA-95064, USA*
[7] *GCI, Soldiers Grove, Wisconsin, 54655.*
[8] *Instituto de Geografía, Facultad de Historia, Geografía y Ciencia Política, Pontificia Universidad Católica de Chile, Chile*
[9] *Kenex Ltd, New Zealand*

Corresponding author: Kaplan at mkaplan@ldeo.columbia.edu; contact info above.

Abstract

We present a comprehensive ^{10}Be chronology for Holocene moraines in the Lago Argentino basin, on the east side of the South Patagonian Icefield. We focus on three different areas, where prior studies show ample glacier moraine records exist because they were formed by outlet glaciers sensitive to climate change. The ^{10}Be dated records are from the Lago Pearson, Herminita Península-Brazo Upsala, and Lago Frías areas, which span a distance of almost 100 km adjacent to the modern Icefield. New ^{10}Be ages show that expanded glaciers and moraine building events occurred at least at 6,120±390 (n=13), 4,450±220 (n= 7), ~1,450 or 1,410±110 (n=18), 360±30 (n=5), and 240±20 (n=8) years ago. Furthermore, other less well-dated glacier expansions of the Upsala Glacier occurred between 1,400 and ~1,000 and ~2,300 and ~2,000 years ago. The most extensive glaciers occurred over the interval from ~6,100 to ~4,500 years ago, and their margins over the last ~600 years were well within and lower than those in the middle Holocene. The ^{10}Be ages agree with ^{14}C-limiting data for the glacier histories in this area.

We then link southern South American, adjacent South Atlantic, and other Southern Hemisphere records to elucidate broader regional patterns of climate and their possible causes. In the early Holocene, a far southward position of the westerly winds fostered warmth, small Patagonian glaciers, and reduced sea ice coverage over the South Atlantic. Although we infer a pronounced southward displacement of the westerlies during the early Holocene, these conditions did not occur throughout the southern mid-high latitudes, an important exception being over the southwest Pacific sector. Subsequently, a northward locus and/or expansion of the winds over the Patagonia-South Atlantic sector promoted the largest glaciers between ~6,100 and ~4,500 years ago and greatest sea ice coverage. Over the last few millennia, the South Patagonian Icefield has experienced successive century-scale advances superimposed on a long-term net decrease in size. Our findings indicate that glaciers and sea ice in the Patagonian-South Atlantic sector of the Southern Hemisphere did not achieve their largest Holocene extents over the last millennium. We conclude that a pattern of more extensive Holocene ice prior to the last millennium is characteristic of the Southern Hemisphere middle latitudes, which differs from the glacier history traditionally thought for the Northern Hemisphere.

1. Introduction

In pioneering work, Mercer (1968) inferred that during the Holocene glaciers in Patagonia may have been larger before the last millennium. He reasoned that, if correct, then such glacier behavior must be related to climates far from Northern Hemisphere influences, where he assumed that Holocene maxima occurred during the European Little Ice Age. In Europe, over the last ~1000 years glaciers were at, or very close to, their maximum Holocene extents (e.g., Grove, 2004; Holzhauser et al., 2005; Davis et al., 2009; Schimmelpfennig et al., 2012), and the conventional wisdom is that this period contained generally the most persistent cold conditions of the epoch (Davis et al., 2009; Kaufman et al., 2009). However, it still remains unclear (e.g., IPCC, 2014) whether the Southern Hemisphere contains different expressions of Holocene glacier-climate from that in the Northern Hemisphere.

In Patagonia, as elsewhere, hypotheses such as Mercers' have been difficult to test robustly, because glacier deposits are difficult to date. ^{14}C dating is commonly used to construct Quaternary glacier chronologies. Although invaluable, this approach often only provides minimum limiting, and less commonly maximum limiting, ages for glacier landforms because they typically lack fossil matter. Moreover, when trying to resolve decadel-multidecadal glacier fluctuations over the last ~500 years, global ^{14}C variations may not permit assignment of unique ages, increasing the uncertainty of the dating approach (e.g., Stuiver, 1978; Porter, 1981).

To this end, we obtained >80 ^{10}Be surface exposure ages that are used to reconstruct Holocene fluctuations of South Patagonian Icefield outlet glaciers (Figs. 1, 2). We use recent advances in the ^{10}Be method (Schaefer et al., 2009) to date directly for the first time the exposure ages of moraine boulders and thus former glacier positions in Patagonia throughout the Holocene, including those that are <500 years old. We targeted the Lago Argentino area for study for several

reasons. First, prior efforts documented which specific glaciers are particularly sensitive to climate and have left the most thorough landform and stratigraphic archives (e.g., Mercer, 1968, Strelin et al., 2014). Earlier studies carried out detailed mapping, stratigraphic studies, and ^{14}C based reconstructions (Mercer, 1968, Aniya, 1995, 2013; Aniya and Sato, 1995; Aniya et al., 1997; Malagnino and Strelin, 1992; Strelin et al., 2011, 2014). This study differs in approach from these valuable prior efforts, as we focus primarily on ^{10}Be dating directly moraine boulders throughout the basin. In particular, we build on the recent work of Strelin et al. (2011, 2014), which demonstrated that in the Lago Argentino basin two independent dating approaches can indeed be used, ^{14}C and ^{10}Be, totaling the confidence and information obtained using both chronologies (Figs. 2-5). For example, combining both approaches allows 1) information on times of glacier expansion (^{10}Be) and retraction (^{14}C); 2) replication of glacial-event ages within a given valley, including knowledge of the bounds of limiting ^{14}C ages; and 3) additional tests of the apparent similarities and differences between valleys.

We then use the record in Patagonia to review broader patterns of paleoclimate in the middle latitudes, by linking the findings with records from the adjacent, downwind, South Atlantic Ocean. Core TN057-13 is near the southern side of the Antarctic Polar front and northern limit of sea ice (Fig. 1). This core thus affords records of sea ice, oceanographic, and climatic conditions also at higher latitudes than just at the drilling site (Kanfoush et al., 2000; Anderson et al., 2009; Divine et al., 2010). By ascertaining similarities between the terrestrial and marine realms, broader hemispheric patterns are reasonably inferred because it can be shown a regional climate change was not only experienced in southern Patagonia. Moreover, we compare our terrestrial-marine based findings with other records in the southern middle latitudes, including of the glacier history in New Zealand, to obtain a hemispheric-wide view.

2. Background and Methods

Mountain glaciers respond sensitively to climate and they are well suited for past climate studies. In particular, glaciers in Patagonia respond directly to atmospheric conditions associated with the globally important Southern Hemisphere Westerly winds and Polar ocean-air climate systems (Fig. 1). 20th/21st century observations document that on timescales of several decades summer temperature dominates glacier history, with precipitation important locally and on the shorter-term (Rignot et al., 2003; Oerlemans, 2005; Rivera and Casassa, 2004; Naruse, 2006; Carrasco et al., 2008; Willis et al., 2012; Casassa et al., 2014). Also, Patagonian glaciers react rapidly to even small changes in climate given the temperate setting. This has led Patagonia to contain some of the fastest waning ice masses in the Southern Hemisphere at present (Rignot et al., 2003; Willis et al., 2012; Casassa et al., 2014).

2.1. Lago Argentino

The regional geology and climate of the Lago Argentino basin, south-central Patagonia, are summarized in detail in Strelin et al. (2011, 2014) and other works (e.g., Aniya, 1995). Two prominent landform complexes are found in the basin, which are informally named Pearson 1 and 2, with the former occurring up to several kilometers beyond the latter (Fig. 2) (Mercer, 1968; Strelin et al., 2014). Sequences of moraines of different ages are preserved at Lago Argentino, because subsequent ice front limits were less extensive and obliteration did not occur, and also they were not eroded by later outwash or river systems. Data from several sites allow us to reproduce our findings (Figs. 2, 3) and see which dated landforms are preserved in respective valleys. For the glacier lobes we focus on in this study, moraines and subaerial outwash plains document that the ice margins were land-terminating or terrestrial based, except for a small section,

116 which is the right (west) lateral margin of Upsala Glacier that presently faces Brazo Upsala (Fig.
117 2). Hence, calving processes are not an issue for our interpretations, given a focus on moraines
118 associated with such subaerially formed features (e.g., also mapped fluvial channels, Fig. 3).

119 The ^{10}Be samples came from large boulders embedded in the crests of moraine ridges that
120 appear stable. All boulders were photographed (e.g., Fig. 4) and their heights measured relative to
121 the ground. For the most part, we sampled boulders at least 50 cm above the moraine matrix. We
122 interpret the ages on boulders rooted on the surfaces of moraine ridges as representing the
123 culmination of its construction, close to the end of a cold period and before onset of retreat due to
124 warming. We sampled hard rhyo-dacitic and granitic boulders. Samples were taken from the upper
125 1-3 cm from the most stable flattish section of the boulder top, with a hammer and chisel or a drill.
126 The azimuthal elevations of the surrounding landscape were measured using a compass and
127 clinometer. We used either a Trimble ProXH GPS system or a handheld Garmin, relative to the
128 WGS 1984 datum, to measure position and altitude. Measurements were relative to benchmark
129 datums near El Calafate established by the Argentine Military. Post processed uncertainites (1σ)
130 were less than 50 cm for the Trimble system and <10 meters (assumed) for the handheld;
131 comparison of Trimble and handheld measurements at the same location typically agree within
132 ~10 m. All samples were processed at the Cosmogenic Nuclide Laboratory at Lamont-Doherty
133 Earth Observatory (Tables S1 and S2). We followed standard geochemical processing protocols
134 explained in Schaefer et al. (2009) and Kaplan et al. (2011). Previously, Strelin et al. (2014)
135 published 15 ^{10}Be ages as an outline of the glacier history.

136 Of crucial relevance for this paper, recent developments enable measurement of ^{10}Be
137 concentrations of only 10^3 atoms/g for the first time in Patagonia. The method advances are
138 summarized in Schaefer et al. (2009) and briefly, include: 1) 'custom-made' low process blanks

139 made from deep mine beryl crystal, the details of which are provided in the Supplementary
140 Material; and 2) recent developments at the Center of Accelerator Mass Spectrometry at Lawrence
141 Livermore National Laboratory that make it possible to measure the low ^{10}Be concentrations. A
142 custom-designed ion source produced high ^{9}Be ion currents ranging typically from 10 to 20 uA
143 for the samples presented in Figure 3.

144 Additional analyses are presented in the Supplementary Material, where it is shown that
145 different statistical central tendencies, i.e., mean, median, and associated errors, notably provide
146 the same finding. The overall coherence of the datasets indicates that geological or geomorphic
147 processes such as erosion or inheritance have minimal effects on these samples (i.e., within 1-2σ
148 uncertainty), except for obvious outliers. Given the relatively youth of the moraines, that is, less
149 than ~6 ka for all samples, we assume erosion has had negligible effect, which is supported by our
150 observations of boulder quality and characteristics (e.g., striations) in the field. For the arithmetic
151 mean ages of the moraines discussed in the main text, we choose to present a conservative error,
152 i.e., including that for the analytical AMS measurement and the production rate.

153 We minimize systematic uncertainties by using a recently-established, high-precision ^{10}Be
154 production rate from the study area (Kaplan et al., 2011). This production rate is statistically
155 indistinguishable from that in New Zealand, also in the middle latitudes of the Southern
156 Hemisphere (Putnam et al., 2010). In Table S2, we provide ages according to the different currently
157 accepted scaling schemes (Balco et al., 2008), although given a local calibration and low elevations
158 and the latitude, ages between the various formulations agree within analytical uncertainties and
159 thus do not alter our findings.

160 Last, all ^{10}Be ages are presented relative to the year of collection (e.g., FR-07-04 is 6,190
161 years before 2007; Table S1). Whereas, all ^{14}C years are presented in years before present relative

to 1950 (e.g., ka BP). In this paper, the difference (<60 years) does not change any findings when comparing chronometers, especially in the context of analytical uncertainties, but it is noted.

2.2 TN057-13 records

Details regarding collection, sampling, age models and other methods are summarized in Nielsen et al. (2007) and Anderson et al. (2006, 2009, 2014). Evaluation of lithogenic and biogenic fluxes follow standard protocols as summarized in these references. Core TN057-13 is a 14-meter-long jumbo piston core obtained in 1996 on cruise TN057 aboard the R/V Thomas Thompson. The core is located at 53°S, south of the present-day polar frontal zone and 2° north of the average winter sea ice limit. Data in Figure 6 are from Anderson et al. (2009), except for additional samples analyzed in this study throughout the Holocene. All data from core TN057-13 are archived at the National Climatic Data Center of the National Oceanic and Atmospheric Administration.

3. Results

3.1. Lago Argentino, southern South America

In the northernmost of the three areas (Fig. 2), near Lago Pearson, we dated moraines formed by two outlet lobes of the Upsala glacier flowing east and southeast (Fig. 3A). For both outlet lobes, moraines are steadily younger towards the present ice margin. Samples from the outermost moraine that wraps around the south end of Lago Pearson (Pearson 1a, yellow on Fig. 3A) have ^{10}Be ages of 5,080±90 to 4,250±180 years. In the area of the upper right lateral, two boulders from short outermost moraine ridges yielded older ^{10}Be ages. The relation is unclear between these apparently older preserved crest slivers and the terminal ~5,000-4,000 ka Pearson 1a moraine that wraps around Lago Pearson. Pearson 1b and c moraines returned ages from

2,170±70 to ~1,000 years. Inside the latter, Pearson 1c limit, all moraines formed within the last ~1 ka. This includes unvegetated moraine ridges on the north end of Lago Pearson, where four of the youngest samples dated have ^{10}Be ages of between 250±20 and 270±20 years.

In the second area we focused on, around Herminita Península and Brazo Upsala, (Figs. 2, 3B), moraines formed during southward expansions of the Upsala Glacier. Moraines are steadily younger towards the present ice margin. Specifically, three samples from the outermost moraine have ages of 5,580±170, 4,760±110, and 4,510±150 years. Inboard, Pearson 1b and c moraines returned ^{10}Be ages from 2,130±70 to 1,360±60 years (cf., Lago Pearson in Fig. 3A). And, inside the Pearson 1c limit, all moraines formed within the last ~700 years.

On the west side of Brazo Upsala we dated two right lateral moraines formed along the Upsala Glacier surface (inset on the left side of 3B). The upper Pearson 1c lateral moraine has ^{10}Be ages (n=4) of 1,410±100 to 1,130±50 years. The lower Pearson 2a lateral moraine has ^{10}Be ages (n=4) of 270±30 to 210±20 years. The lateral moraines document that the surface of the Upsala Glacier was at a lower elevation during the last few hundred years, after the higher Pearson 1c moraine formed (i.e., 1,360±30 to 1,130±50 years). In addition, a moraine located southwest of Bahía Onelli, that formed after the Onelli and Upsala Glaciers separated, has two ^{10}Be ages of 1,480±90 and 1,420±80 years (from Strelin et al., 2014).

The third area where we focused ^{10}Be dating is around Lago Frías (Figs. 2, 3C). Here, a prominent outermost moraine complex, locally mapped as Frías 1a, yielded 13 ages with a range from 6,550±200 (and 6,550±150) to 5,360±250 years. Inside this outer ~6 ka limit, a moraine near the south end of Lago Frías has ^{10}Be ages of 5,800±200 and 5,600±200 years; hence, the ^{10}Be ages on either side of Lago Frías are statistically indistinguishable. Closer to the present ice margin,

208 boulders yielded ^{10}Be ages of 530±40 to 140±20 years. Only one outlier is identified (1,110±110)
209 because it violates the relative stratigraphy and all other ages in the inner Frías valley.

210 For the Lago Argentino basin, for the sake of discussion, for the different outlet glaciers
211 we provide average ages only for moraines that are the best dated; that is, with at least four
212 statistically indistinguishable ^{10}Be ages on continuous traceable ridges (details in Supplementary
213 Material). These mark expanded glaciers at 6,120±390 (Frías, n=13, no outliers at 1-2σ),
214 4,450±220 (at Lago Pearson, n= 7), ~1,450±90 ka (Herminita Península-Onelli, n=8), 1,410±110
215 (Lago Pearson, n=8), 360±30 years (on Herminita Península, n=5, no outliers), 260±10 years ago
216 (Lago Pearson, n=4), and 230±20 (Herminita Península-Onelli, n=4). Combining the four
217 youngest ^{10}Be ages at both Lago Pearson (Fig. 3A) and west of Brazo Upsala (Fig. 3B) provides
218 an age of 240±20 years (no outliers), a limit that represents the last major dated advance of the
219 Upsala Glacier (Fig. 1). Individual ^{10}Be ages on other less well-dated moraine ridges at Lago
220 Argentino are consistent with the mean moraine ages provided above. For example, three different
221 outermost moraine crests on the Herminita Península (Fig. 3B) also have three respective ages
222 ranging from 5,580±170 to 4,510±150 years, consistent with Pearson 1a ages around the Lago
223 Pearson and Frías areas (Figs. 3A and C). Interestingly, several of the outliers (e.g., 5080±90, Fig
224 3A; 2210±140, Fig. 3B), although statistically older than the other ages on the crests they are from,
225 are consistent overall with periods of expansion (Fig. 6). Perhaps, at least some of these outliers
226 are on older erratic boulders preserved in landforms that are younger for the most part.

227

228 *3.2. TN057-13 and the southern South Atlantic.*
229
230 Most of the results were discussed in prior papers and here we only briefly review the
231 salient observations, which include new data (Fig. 6) relevant for the Discussion in Section 4. In

core TN057-13, the highest opal fluxes (>6 g/cm^2/ka) are observed during the early Holocene, before ~6 ka, and subsequently values decrease towards 1 g/cm^2/ka for the remainder of the epoch. Also during the early Holocene, lithogenic fluxes exhibit high viability, but this is superimposed on a net increase to almost 0.25 g/cm^2/ka by ~7 ka. After ~ 3 ka, through the reminder of the Holocene, lithogenic fluxes to the South Atlantic generally decreased, although there are notable centennial-scale periods of increase (Fig. 6).

Sea ice fluctuations in the South Atlantic, including latitudinal changes, are discussed in Divine et al. (2010) and include data from TN057-13 (Fig. 6). Overall, there appears to be a positive correlation between sea ice and lithogenic fluxes; and both of these proxies are negatively correlated with opal flux (at least) in the early Holocene. That is, the lowest sea ice values (e.g., months/yr) are in the earliest Holocene, before about 9 ka, when the winter ice edge appears to be consistently south of ~54°S. Towards the middle of the Holocene, although variable, there is a general net increase in months/yr of sea ice. Over the last several thousand years, the amount of sea ice fluctuates between ~1 and 4 months/yr along with maximum winter ice edge latitude. Our findings of a marked change from the early to mid-Holocene, and then relatively sustained values after, are in agreement with earlier, lower resolution results from TN057-13 in Hodell et al.(2001).

4. Discussion

4.1. Lago Argentino

Eighty three ^{10}Be ages allow us to build on the known framework of the glacier history in the Lago Argentino area (Section 1). We highlight that there are no observed Holocene moraines ^{10}Be dated prior to about 6 ka, with a possible exception of two older ^{10}Be ages (8660±180 and 6990±200) on small ridges preserved along the uppermost left lateral at Lago Pearson (Fig. 3A). To decipher the glacier behavior during the earliest Holocene prior to ~6 ka, we turn instead to the

257 complementary ^{14}C chronology (Fig. 5), presented in Strelin et al. (2011, 2014). Their ^{14}C results
258 include maximum-limiting ages on reworked pieces of wood in sediments in stratigraphic sections
259 in Agassiz Este Valley, and on samples from basal sections of bog cores around Lago Anita and
260 Lago Frías (Figs. 3, 5; Table S3; Strelin et al., 2011, 2014). These data indicate that after the Late
261 Glacial advances the South Patagonian Icefield retreated to close to present ice margins (Figs. 3A,
262 C; Strelin et al., 2011, 2014). Any early Holocene advances (e.g., ~8-7 ka, in Strelin et al., 2014)
263 of the glacier margin were within the subsequent maximum expansions (Fig. 3).

264 For the rest of the Holocene, we point out the following glacier patterns. First, a robust
265 finding – reproduced between all sites studied – is that at least three different outlet glaciers of the
266 South Patagonian Icefield exhibit maximum expansions in the middle Holocene, between ~6 ka
267 and ~4.5 ka (Figs. 2, 3). Strelin et al. (2014) defined the middle Holocene expansion from ~6 to 5
268 ka. The ^{10}Be data can be used to infer that either this period persisted longer than previously
269 appreciated, or the younger 4.5 ka event was a subsequent pulse. Second, at all sites glacier
270 advances were smaller in size after ~4.5 ka, and smaller after their limit at ~600-500 years ago.
271 Over the last 600 years, glaciers are far less extensive than their earlier counterparts (Fig. 3).
272 Decreasing ice extents after the middle Holocene are best revealed around Lago Pearson and on
273 the Herminita Península, which have the most comprehensive moraine records, and in the Frías
274 valley (Fig. 3A,B and C). Lateral moraines around Lago Pearson and west of Brazo Upsala also
275 document that the surface of the Upsala Glacier was lower during successive expansions, including
276 at 230±20 years ago (Figs. 3A, B).

277 Overall, the ^{14}C and ^{10}Be data are in agreement, excluding two outliers that occur on
278 moraines on the Herminita Península (1450±80a/1360±60b and 2210±140, Fig. 3B) and one in the
279 lower part of the Frías river valley (1110±110, Fig. 3C). We point out that the two chronometers

do not need to overlap to be consistent. The ^{14}C ages discussed in Strelin et al. (2011, 2014), as well as in earlier studies (e.g., Aniya, 1995, 2013) often only provide minimum- or maximum-limiting ages and thus bracket the timing of moraine building events.

In addition to the common patterns highlighted above, we note that there are some differences between the valleys in terms of dated moraines preserved (Fig. 3). However, we emphasize though that the observed pattern of maximum expansions in the middle Holocene, and smaller successive margins after, are independent of the (secondary) differences between the valleys – these are reproduced patterns over ~100 km of the eastern side of the Icefield (Fig. 3). Strelin et al. (2014) discussed in depth the differences in moraines preserved between valleys and their possible causes. They demonstrated that such differences in preservation can be explained largely by happen chance (e.g. an example is shown in Figure S1d) and variability in hypsometry, which leads to dissimilar glacier sensitivities to a regional climate event and responses in glacier length. In essence, during a given climate change, where the change in equilibrium line altitude (ELA) occurs in relation to glacier hypsometry can determine the magnitude of response in glacier length (Figs. 15 and 16 in Strelin et al., 2014). Mercer (1968) originally discussed that the Upsala Glacier illustrates the key role hypsometry can play, as ELA changes there consistently occur over a low surface gradient, causing a relatively large area to be affected. Hence, it is not surprising that the Upsala Glacier moraines are widely separated and well-preserved at Lago Argentino (Fig. 3B; Mercer, 1968; Strelin et al., 2014). The argument of Strelin et al. (2014) is also partly based on the observation that climate does not vary in a major way over the 100 km along this eastern sector of the Icefield (Fig. 2), and the focus here is on past non-calving glaciers (except for small sections).

4.2. Southern South America

303 Our findings on Patagonian glacier evolution derived from moraines are in agreement with
304 observations from other diverse data sets in southern South America. Paleotemperatures have been
305 estimated in nearby areas for the discrete time periods in which maximum and minimum glacier
306 extents are observed in the Lago Argentino basin. Specifically, before 6 ka, when outlet glaciers
307 were relatively small (Mercer, 1976; Moreno et al., 2009; Strelin et al., 2011. 2014; Menounos et
308 al., 2013), estimates for onshore and offshore temperatures are ~2-3℃ warmer than present (e.g.,
309 Heusser, 1974; Lamy et al., 2010). Additionally, paleoecologic data document that the early
310 Holocene was the warmest and driest part of the epoch, prior to the 20th century (e.g., Moreno and
311 Leon, 2003; Markgraf et al., 2007; Whitlock et al., 2007; Kilian and Lamy, 2012).
312 In the earliest and middle Holocene, evidence for centennial-scale advances also exists
313 both to the north and south of the Lago Argentino area (Mercer, 1976; Douglass et al., 2005;
314 Moreno et al., 2009; Aniya, 2013). Douglass et al. (2005) estimated a ~300 m lowering of the
315 equilibrium line altitude (ELA) at 46°S, corresponding to temperatures ~2 to 3℃ cooler than
316 present (a maximum value if it is wetter as well as colder). The finding of prior efforts, of
317 pronounced middle-early Holocene glacier expansions, much earlier than the last millennium, is
318 consistent with our findings.
319 In the late Holocene, tree-ring and modeling-based temperature reconstructions agree, with
320 estimates about 1 to 2°C colder than present between ~600 and ~200 years ago, with the lowest
321 temperatures earlier in this interval (Villalba et al., 2005). Others have also noted that glaciers in
322 the middle latitudes of South America advanced during the last ~600 years (e.g., Mercer, 1976;
323 Aniya, 1995, 2013; Aniya and Sato, 1997; Kilian and Lamy, 2012; Strelin et al., 2008). However,
324 ^{10}Be dating directly ice marginal limits over the last ~600 years, defined by moraines, reveals that
325 these advances were less expansive than those during the mid Holocene.

326

327 *4.3 South Atlantic - Southern South America*

328 At site TN057-13, opal flux is interpreted to represent a proxy for upwelling in the Southern
329 Ocean, which can be forced by the prevailing westerlies (Anderson et al., 2009). Lithogenic
330 material deposited at the core site is mainly volcanic in origin and transported from the South
331 Sandwich Islands by sea ice (Nielsen et al., 2007). Such material may increase due to sea surface
332 temperature decline and sea ice survival (Anderson et al., 2006, 2009, 2014; Nielsen et al., 2007;
333 Kanfoush et al., 2000; Divine et al., 2010). Regardless of the specific factors regulating changes
334 in the deposition of lithogenic material, its flux reflects sea ice cover, which along with opal flux,
335 are a function of the position of the westerly wind belt. That is, the position of the westerlies and
336 the winter ice extent are positively correlated (e.g., equatorward westerlies = equatorward ice
337 edge). Hence, we equate less (or more) sea ice with a southward (northward) displacement of the
338 winds. We assume southward/northward displacement of the winds (or intensity) may be also
339 associated with contraction/expansion of the wind belt, although our data alone cannot address
340 such dynamics (e.g., Lamy et al., 2010; Björck et al., 2012).

341 Given that the South Atlantic Ocean and adjacent southern Patagonia are at a similar
342 latitude and affected by the core of the westerly wind belt (Fig. 1) (e.g., Villalba et al., 1997; Yuan
343 and Martinson et al., 2000; Stammerjohn et al., 2008), linking the terrestrial record with marine-
344 based findings can reveal paleoclimate outlines that are regionally coherent over a broad swath of
345 the southern latitudes. (Fig. 6). We first highlight that we are mainly pointing out broad patterns
346 and we are not necessarily focusing on correlating short-term individual peaks or events (e.g., less
347 than a century), given differences between proxy types and some spatiotemporal variability might
348 be expected. During the early Holocene, peak opal fluxes (Anderson et al., 2009) imply a far

349 southerly position of the westerlies, which explains a climatic optimum with warm and dry
350 conditions over the southern Andes (e.g., Moreno and Leon, 2003; Whitlock et al., 2007; Kilian
351 and Lamy, 2012), causing glaciers to be similar to or behind present limits (Figs. 3, 5; Strelin et
352 al., 2014). Perhaps the early Holocene is an analog for a warmer future in Patagonia. Before ~6
353 ka, lithogenic fluxes in TN057-13 exhibit high variability, but this is superimposed on a net
354 increase (Fig. 6). Subsequently, the greatest sea ice coverage in the South Atlantic over the
355 Holocene, as indicated by months/yr and lithogenic flux reconstructions (Fig. 6), was over the time
356 interval of the most extensive outlet glaciers, from ~6 to ~4.5 ka. Both South American and South
357 Atlantic data are consistent therefore with colder air over these latitudes (~50-55°S) during the
358 middle Holocene, when supposedly the westerly winds are more equatorward compared with the
359 early part of the epoch. Our conclusions are in agreement with those in an earlier study in the South
360 Atlantic by Hodell et al (2001). Paleoecologic data are consistent with this finding (e.g., Markgraf
361 et al., 2007; Whitlock et al., 2007; Schäbitz et al., 2013). After the middle Holocene, over the last
362 few thousand years, the findings from the South Atlantic and southern Patagonia indicate cold
363 conditions generally remain sustained. There is a notable gap in dated moraines between ~4 and
364 ~3 ka, which may imply glaciers were small at this time, or instead, any expansions were just
365 inside the subsequent limit and not preserved. For the Holocene, the data also may imply the
366 westerlies do not exhibit their early Holocene position in a persistent manner again (until the 20th
367 century), and perhaps fluctuate between settings reached in the early and middle parts of the epoch.
368 For comparison to the findings shown on Figure 6, we also mention other observations
369 closer to southernmost South America (Fig. 7) and in the South Atlantic Ocean. We are not aware
370 of high-resolution records for the entire Holocene from ocean sediments in the South Atlantic
371 nearer to Patagonia (i.e., west of TN057), or in the Pacific away from the Chile shelf, within the

latitude band of our records (~50-53°S) and the core of the westerlies. On the Pacific side of Patagonia, Lamy et al. (2010) studied a range of proxies for wind strength and precipitation in fjords and adjacent land bogs. On the South Atlantic side, as no high resolution records are available closer to southern Patagonia, instead, we present recent results from Björck et al. (2012), who inferred wind changes from deposition of locally-derived coarse grained lithogenic material on Isla de los Estados, ~55°S (building on prior studies, such as Ponce et al., 2011).

Before discussing comparisons between records, we first emphasize that we agree with the conclusion of Björck et al. (2012) that differences between records (especially distinct 'events') could be primarily due to what the proxies imitate and the seasons they represent. Also, the sensitivity of a proxy to changes in westerly strength could vary depending on where the core of the winds are located relative to the site (e.g., Figs. 7b, 7c). Nonetheless, for the sake of discussion, some broad patterns between records are highlighted. Notably, all records on Figure 7 are consistent with the interpretation that the westerly winds are displaced far southward during the early Holocene. Lamy et al. (2010) inferred that perhaps (analogues) characteristics of the westerlies during the modern summer and winter typified the early and late Holocene, respectively. Subsequently, they shift back north by the middle Holocene. For the remainder of the Holocene, other paleoclimate records shown on Figure 7 are consistent with our inference that the westerlies fluctuated between their early and middle Holocene positions. In addition, after recently synthesizing available data for the last ~30 ka from the South Atlantic Ocean, irrespective of the resolution, Xiao et al. (2016) also inferred southward displacement of the westerlies and early Holocene warmth, and subsequently, a generally more northward position for the rest of the epoch. Nonetheless, how the winds shift, that is, whether a displacement and/or contraction/expansion, remains an open question (Björck et al., 2012).

395

396 *4.4 Other Southern Hemisphere comparisons*

397

398 Briefly, we also compare past glacier behavior at the middle latitudes on both sides of the
399 South Pacific Ocean - that is, the same type of proxy record that is largely responsive to summer
400 conditions. Outside the sub Antarctic realm, New Zealand is the other major landmass in the
401 middle latitudes of the Southern Hemisphere, besides South America, that contains glacier
402 records for the last ~11,500 years (e.g., Grove, 2004; Kirkbride and Winkler, 2012; Schaefer et
403 al., 2009; Solomina et al., 2015). As discussed in Sections 4.1-4.3, in the early Holocene glaciers
404 are generally retracted in the warm dry Southern Andes (Moreno and Leon, 2003), with South
405 Atlantic evidence in agreement and implying southward displacement (and perhaps contraction
406 to higher southern latitudes) of the westerlies over this sector of the hemisphere (Fig. 6). In
407 contrast, in New Zealand the lowest ELAs and maximum glacier expansions are observed during
408 the early Holocene (Putnam et al., 2013; Kaplan et al., 2013). Also, when southern Patagonian
409 ice fronts are most extensive between ~6 and 4.5 ka, for comparison, glaciers in New Zealand are
410 behind their earlier Holocene maxima (Gellatly et al., 1988; Schaefer et al., 2009; Putnam et al.,
411 2013; Kaplan et al., 2013).

412 To explain the possible cause of early Holocene (as well as later in the Epoch) climate
413 similarities and differences across the middle latitudes of the Southern hemisphere, we offer the
414 following testable hypothesis. Over the last few decades, there have been opposing regional
415 trends in mean climate states between the Antarctic Península/southern Bellingshausen Sea and
416 the western Ross Sea region, with contrasting temperatures, sea ice duration and concentrations
417 (Yuan and Martinson, 2000; Stammerjohn et al., 2008). A strong Antarctic dipole reflects an out-
418 of-phase relationship between the central/eastern Pacific and Atlantic sectors of the Antarctic

(Pittock, 1980; Yuan and Martinson, 2000). Such patterns can be explained based on the eccentricity of the circulation or polar vortex around the South Pole (Fig. 8). We infer that sustained modes of relatively high eccentricity of the polar vortex during the early Holocene, similar to that of the last few decades (Fig. 8), typically favored a weak subtropical jet and a strong polar front jet in the Southern Hemisphere. In the early Holocene this caused warm winds and less sea ice around the South Atlantic-Weddell Sea sector (Section 4.3), but the opposite in the southwest Pacific sector including around New Zealand. Also, during this time New Zealand was likely affected by the relatively cool up-wind East Australian Current, linked to the behavior of the West Pacific Warm Pool and tropical climates (Fig. 1) (Putnam et al., 2012). Moreover, given the higher latitudes of southern Patagonia, its climate may have been influenced by the far southward westerlies acting in concert with the duration of summer insolation, near the sea ice edge (Huybers and Denton, 2008). We speculate that, perhaps, a corollary is that the polar vortex and circulation around the South Pole was less eccentric (similar regional trends in mean climate states) during cold events of the last ~600 years, when glaciers on both sides of the Pacific Ocean appear to have advanced repeatedly (e.g., Gellatly et al., 1988; Kirkbride and Winkler, 2012; Schaefer et al., 2009; Putnam et al., 2013; Kaplan et al., 2013; Solomina et al., 2015).

We also point out another possible implication of a relatively eccentric polar and westerly circulation in the early Holocene. Prior to the Holocene, southward displacement of the westerly winds appears to occur with cold Northern Hemisphere stadials, such as during deglacial time, ~18 ka to 15 ka (Denton et al. 2010). The early Holocene may present a different scenario, whereby, parts of the mid to high southern latitudes instead experience southward displacement of the winds during Northern Hemisphere nonstadial or interglacial climates, in association with an eccentric polar and Westerly circulation. Future observations and modeling experiments can

test such ideas, for example, on the effects of eccentricity of polar circulation and westerly winds in past climates.

5. Conclusions

Cosmogenic ^{10}Be dating directly on Holocene morainal landforms allows new insights into glacial histories in Patagonia, building on prior studies that have had to rely mainly on limiting ^{14}C ages. Furthermore, when the terrestrial South American record is linked with marine South Atlantic findings, this reveals paleoclimate patterns that were quasi-hemispheric. The Patagonian-South Atlantic view of the early Holocene is a time of general warmth, and dry conditions over the southern Andes, with retreated glaciers. Afterwards, glacial and marine-based records collectively are in agreement that colder conditions characterized the middle Holocene. A sustained northward displacement of the westerly wind belt (intensity and/or expansion) during the middle Holocene is compatible with the largest glacial expansions and sea ice concentrations. As in prior works, we observe advances during the last ~600 years (e.g., Mercer, 1976; Aniya, 1995, 2013; Aniya and Sato, 1997; Kilian and Lamy, 2012; Strelin et al., 2008, 2014). However, directly dating former glacier limits defined by landforms, based on the exposure duration of its constituent boulders, reveals that these advances were less expansive than during the middle Holocene.

From a broader perspective, there appear to be differences and similarities between paleoclimatic records across the middle latitudes of the Southern Hemisphere. On the one hand, glacier and marine based evidence suggest out-of-phase patterns between the Patagonia/South Atlantic and New Zealand/southwest Pacific sectors, during the earliest Holocene. Perhaps, these differences can be explained by invoking comparison with 20th/21st century opposing regional trends in mean climate states around the mid-high southern latitudes (e.g., Yuan and Martinson,

2000; Stammerjohn et al., 2008). Specifically, we hypothesize perpetual modes of relatively high eccentricity of the polar vortex, similar to that of the last few decades, favored warm winds and less sea ice around the South Atlantic-Weddell Sea, but the opposite in the southwest Pacific sector. On the other hand, a common finding is that during the Holocene glaciers on both sides of the South Pacific Basin were not the largest during the last millennium. Sea ice proxies from the South Atlantic Ocean are consistent with the glacier moraine based evidence. This raises the question of the degree to which glacier (or cyrospheric) histories in the Southern Hemisphere are categorically analogues to defined patterns of Little Ice Age behavior in the Northern Hemisphere.

Appendix A. Supplementary data. Supplementary data related to this article can be found at http:XXXXX.

Acknowledgements. The research herein represents almost a decade of efforts by many individuals, which must be recognized. We are grateful to the Comer Science and Education Foundation), Instituto Antartico Argentino (IAA), Centro de Investigaciones en Ciencias de la Tierra (CICTERRA), NOAA, NSF EAR-0902363, funded through the American Recovery and Reinvestment Act of 2009 (ARRA), and the Climate Center of LDEO and NASA GISS. Analysis of the Holocene portion of TN057-13 were supported by a grants/ cooperative agreement from the National Oceanic and Atmospheric Administration. The views expressed herein are those of the authors and do not necessarily reflect the views of NOAA or any of its sub-agencies. Marcus Vandergoes was supported by the New Zealand Government through the GNS Global Change through Time Programme. Geol Cesar Torielli from Cordoba University (UNC) and numerous students from UNC who assisted us during the field work. For logistical support we thank Alejandro Tur and for discussion Aaron Putnam and Patricio Moreno. We thank Patricia Malone and Martin Fleisher for opal and thorium analyses, respectively, in TN057-13. Also, we are grateful to Hielo & Aventura (Jose Pera), Estancia Cristina (Daniel Moreno), Estancia La Querencia (Pedro Manger) and Administracion de Parques Nacionales (Guardaparque Fernando Spikermann). Last we thank Maarten Van Daele and an anonymous reviewer for helping us to improve substantially the manuscript. This is Lamont-Doherty Earth Observatory Contribution XXXX.

References

Anderson, R.F., Fleisher, M.Q., Lao, Y., 2006. Glacial-interglacial variability in the delivery of dust to the central equatorial Pacific Ocean. Earth and Planetary Science Letters 242, 406-414.

Anderson, R.F. Ali, S., Bradtmiller, L.I., Nielsen, S.H.H, Fleisher M.Q., Anderson, B.E., Burckle, L.H., 2009. Wind-Driven Upwelling in the Southern Ocean and the Deglacial Rise in Atmospheric CO_2. Science 323, 1443-1448.

Anderson, R.F., Barker, S., Fleischer, M., Gersonde, R., Goldstein, S.L., Kuhn, G., Mortyn, P.G., Pahnke, K., Sachs, J.P., 2014. Biological response to millennial variability of dust and nutrient supply in the Subantarctic South Atlantic Ocean. Philosophical Transactions of the Royal Society A: Mathematical, Physical and Engineering Sciences 372, doi.org/10.1098/rsta.2013.0054.

Aniya, M., 1995. Holocene glacial chronology in Patagonia: Tyndall and Upsala Glaciers. Arctic and Alpine Research 27, 311-322.

Aniya, M., 2013. Holocene glaciations of Hielo Patagónico (Patagonia Icefield), South America: a brief review. Geochemical Journal 47, 97-105.

Aniya, M., Sato, H., 1995. Holocene glacial chronology of Upsala Glacier at Peninsula Herminita, Southern Patagonia Icefield. Glacier research in Patagonia. Bulletin of Glacier Research 13, 83-96.

Aniya, M., Sato, H., Naruse, R., Skvarca, P., Casassa, G., 1997. Recent glacier variations in the Southern Patagonia Icefield, South America. Arctic and Alpine Research 29, 1-12.

Balco, G., Stone, J.O, Lifton, N.A., Dunai, T.J.A., 2008. A complete and easily accessible means of calculating surface exposure ages or erosion rates from ^{10}Be and ^{26}Al measurements. Quaternary Geochronology 3, 174-195.

Bevington, P., Robinson, D., 2003. Data Reduction and Error Analysis for the Physical Sciences. WCB McGraw-Hill, New York, 320 pp.

Carrasco, J.F., Osorio, R., Casassa, G., 2008. Secular trend of the equilibrium-line altitude on the western side of the southern Andes, derived from radiosonde and surface observations. Journal of Glaciology, 54, 538-550.

Casassa, G., Rodriguez, J., Loriaux, T., 2014. A new glacier inventory for the Southern Patagonia Icefield and areal changes 1986–2000. Global Land Ice Measurements from Space. Springer Praxis Books, 639-660.

Denton, G.H., Anderson, R.F., Toggweiler, J.R., Edwards, R.L., Schaefer, J.M., Putnam, A,E, 2010. The Last Glacial Termination. Science. 328, 1652-1656.

Davis, P.T., Menounos, B.A., Osborn, G., 2009. Holocene and latest Pleistocene alpine glacier fluctuations: A global perspective. Quaternary Science Reviews 28, 2021-2033.

Desilets, D., Zreda, M., 2003. Spatial and temporal distribution of secondary cosmic-ray nucleon intensities and applications to in-situ cosmogenic dating. Earth and Planetary Science Letters 206, 21-42.

Divine, D.V., Koc, N., Isaksson, E., Nielsen, S., Crosta, X., Godtliebsen, F. 2010. Holocene Antarctic climate variability from ice and marine sediment cores: Insights on ocean-atmosphere interaction. Quaternary Science Reviews 29, 303-312.

Douglass, D. C., Singer, B.S., Kaplan, M.R., Ackert, R.P., Mickelson, D.M., Caffee, M.W., 2005. Evidence of Early Holocene Glacial Advances in Southern South America from Cosmogenic Surface Exposure Dating. Geology 33, 237-240.

Dunai, T.J., 2001. Influence of secular variation of the magnetic field on production rates of in situ produced cosmogenic nuclides. Earth and Planetary Science Letters 193, 197-212.

Gellatly, A.F., Chinn, T.J.H., Rothlisberger, F., 1988. Holocene glacier variations in New Zealand: a review. Quaternary Science Reviews 7, 227-242.

Grove, J.M., 2004, Little Ice Ages: Ancient and modern: London, New York, Routledge, 718 p.

Heusser, C.J., 1974. Vegetation and climate of the southern Chilean Lake District during and since the last interglaciation, Quaternary Research 4, 290–315.

Holzhauser, H., Magny, M., and Zumbühl, H.J., 2005. Glacier and lake-level variations in west-central Europe over the last 3500 years. The Holocene 15, 789–801,

Hodell, D., Kanfoush, S., Shemesh, A., Crosta, X., Charles, C., Guilderson, T., 2001. Abrupt cooling of Antarctic surface waters and sea ice expansion in the south Atlantic sector of the southern ocean at 5000 cal yr B.P. Quaternary Research 56, 191–198.

Huybers, P., Denton, G.H., 2008. Antarctic temperature at orbital timescales controlled by local summer duration. Nature Geosciences 1, 787–792.

IPCC, 2014. Climate Change 2013: The Physical Science Basis. Contribution of Working Group I to the Fifth Assessment Report of the Intergovernmental Panel on Climate Change, 1552 pp.

Kaufman, D.S., Schneider, D.P., McKay, N.P., Ammann, C.M. & Bradley, R. et al., 2009. Recent warming reverses long-term Arctic cooling. Science 325, 1236-1239.

Kilian, R., Lamy, F., 2012. A review of Glacial and Holocene paleoclimate records from southernmost Patagonia (49-55°S). Quaternary Science Reviews 53, 1-23.

591 Kanfoush, S.L., Hodell, D.A., Charles, C.D., Guilderson, T.P., Mortyn, P.G., Ninnemann, U.S.,
592 2000. Millennial-scale instability of the Antarctic ice sheet during the last glaciation. Science 288,
593 1815-1818.
594
595 Kaplan, M.R., Strelin, J.A., Schaefer, J.M., Denton, G.H., Finkel, R.C., Schwartz, R., Putnam,
596 A.E., Vandergoes, M.J., Goehring, B.M., Travis, S.G., 2011. In-situ cosmogenic ^{10}Be production
597 rate at Lago Argentino, Patagonia: Implications for late-glacial climate chronology. Earth and
598 Planetary Science Letters 309, 21-32.
599
600 Kaplan, M.R., Schaefer, J.M., Denton, G.H., Doughty, A.M., Barrell, D.J.A., Chinn, T.J.H.,
601 Putnam, A.E., Andersen, B., Mackintosh, A.N., Finkel, R.C., Schwartz, R., Anderson, B.A., 2013.
602 The anatomy of 'long-term' warming since 15 kyr ago in New Zealand based on net glacier
603 snowline rise. Geology 41, 887-890.
604
605 Kaufman, D.S., Schneider, D.P., McKay, N.P., Ammann, C.M., Bradley, R. et al., 2009. Recent
606 warming reverses long-term Arctic cooling. Science 325, 1236-1239.
607
608 Kirkbride, M.P., Winkler, S., 2012. Timescales of climate variability, glacier response, and
609 chronological resolution: Issues for correlation of late Quaternary moraines. Quaternary Science
610 Reviews 46, 1–29.
611
612 Mercer, J., 1968. Variations of some Patagonian glaciers since the late glacial I. American Journal
613 of Science 266, 91-109.
614
615 Lamy, F. Kilian, R., Arz, H.W., Francois, J.-P., Kaiser, J., Prange, M., Steinke, T., 2010. Holocene
616 changes in the position and intensity of the southern Westerly wind belt. Nature Geoscience 3,
617 695-699.
618
619 Lifton, N., Smart, D., Shea, M. 2008. Scaling time-integrated in situ cosmogenic nuclide
620 production rates using a continuous geomagnetic model. Earth and Planetary Science Letters 268,
621 190-201.
622
623 Malagnino, E., Strelin J., 1992. Variations of Upsala Glacier in southern Patagonia since the late
624 Holocene to the present. In: Naruse, R. and Aniya, M. (eds), Glaciological Researches in
625 Patagonia, 1990, 61-85. Japanese Society of Snow and Ice.
626
627 Menounos, B., Clague, J.J., Osborn, G, Davis, P.T., Ponce, F., Goehring, B.M., Maurer, M.,
628 Rabassa, J., Coronato, A., Marr, R., 2013. Latest Pleistocene and Holocene glacier fluctuations in
629 southernmost Tierra del Fuego, Argentina. Quaternary Science Reviews 77, 70-79.
630
631 Mercer, J., 1976. Glacial History of Southernmost South America. Quaternary Research 6, 125-
632 166.
633
634 Moreno, P.I., Leon, A.L., 2003. Abrupt vegetation changes during the last glacial to Holocene
635 transition in mid-latitude South America. Journal of Quaternary Science 18, 787-800.
636

637 Moreno, P.I., Francois, J.P., Villa-Martinez, R.P., Moy, C.M., 2009. Millennial-scale variability
638 in Southern Hemisphere westerly wind activity over the last 5000 years in SW Patagonia.
639 Quaternary Science Reviews 28, 25-38.
640
641 Naruse, R., 2006. The response of glaciers in South America to environmental change, In Glacier
642 Science and Environmental Change. Blackwell Publishing, Oxford, pp. 231-238.
643
644 Oerlemans, J., 2005. Extracting a Climate Signal from 169 Glacier Records. Science 29, 675-
645 677.
646
647 Pigati, J. S., Lifton, N. A., 2004. Geomagnetic effects on time-integrated cosmogenic nuclide
648 production with emphasis on in situ ^{14}C and ^{10}Be. Earth and Planetary Science Letters 226, 193-
649 205.
650
651 Pittock, A.B., 1980. Patterns of climatic variation in Argentina and Chile I. Precipitation, 1931-
652 1960. Monthly Weather Review 108, 1347–1361.
653
654 Ponce, J.F., Borromei, A.M., Rabassa, J., Martinez, O., 2011. Late Quaternary
655 palaeoenvironmental change in western Staaten island (54.5°S, 64°W), Fuegian Archipelago.
656 Quaternary International 233, 89-100.
657
658 Porter, S.C., 1981. Glaciological evidence of Holocene climatic change. In Wigley, T.M.L.,
659 Ingram, M.J. and Farmer, G., editors, Climate and History Studies on Past Climates and their
660 Impact on Man. Cambridge: Cambridge University press, 82–110.
661
662 Putnam, A., Schaefer, J., Barrell, D.J.A., Vandergoes, M., Denton, G.H., Kaplan, M., Finkel,
663 R.C., Schwartz, R., Goehring, B.M., Kelley, S., 2010. In situ cosmogenic ^{10}Be production-rate
664 calibration from the Southern Alps, New Zealand. Quaternary Geochronology,
665 doi:10.1016/j.quageo.2009.12.001.
666
667 Putnam, A.E., Schaefer, J.M., Denton, G.H., Barrell, D.J.A., Finkel, R.C., Andersen, B.G.,
668 Schwartz, R., Chinn, T.J.H., Doughty, A.M., 2012. Regional climate control of glaciers in New
669 Zealand and Europe during the pre-industrial Holocene. Nature Geoscience 5, 627-630.
670
671 Rignot, E., Rivera, A., Casassa, G. Contribution of the Patagonia Icefields of South America to
672 Sea Level Rise, Science 302, 434-436.
673
674 Rivera, A., Casassa, G., 2004. Ice Elevation, Areal, and Frontal Changes of Glaciers from National
675 Park Torres del Paine, Southern Patagonia Icefield Arctic, Antarctic, and Alpine Research 36,
676 379–389.
677
678 Schäbitz, F., Wille, M., Francois, J.-P., Haberzettl, T., Quintana, F., Mayr, C., Lücke, A.,
679 Ohlendorf, C., Mancini, V., Paez, M.M., Prieto, A.R., Zolitschka, B., 2013. Reconstruction of
680 paleoprecipitation based on pollen transfer functions – the record of the last 16 ka from Laguna
681 Potrok Aike, southern Patagonia. Quaternary Science Reviews 71, 175-190.
682

683 Schaefer, J.M., Denton, G.D., Kaplan, M. R., Putnam, A., Finkel , R.C., Barrell, D.J.A., Andersen,
684 B.G., Schwartz, R. Mackintosh, A., Chinn, T., Schlüchter, C., 2009. High-Frequency Holocene
685 Glacier Fluctuations in New Zealand Differ from the Northern Signature. Science 324, 622-625.
686
687 Schimmelpfennig, I., Schaefer, J.M., Akçar, N., Ivy-Ochs, S., Finkel, R.C., and Schlüchter, C.,
688 2012. Holocene glacier culminations in the Western Alps and their hemispheric relevance.
689 Geology 40, 891–894.
690
691 Solomina, O., Bradley, R.S., Hodgson, D.A., Ivy-Ochs, S., Jomelli, V., Mackintosh, A.N., Nesje,
692 A., Owen, L.A., Wanner, H., Wiles, G.C., Young, N.E., 2015. Holocene glacier fluctuations.
693 Quaternary Science Reviews 111, 9-34.
694
695 Stammerjohn, S.E., Martinson, D.G., Smith, R.C., Yuan, X. & Rind, D. Trends in Antarctic annual
696 sea ice retreat and advance and their relation to El Niño-Southern Oscillation and Southern
697 Annular Mode variability. J. Geophys. Res. 108 (2008).
698
699 Strelin, J., Casassa, G., Rosqvist, G., Holmlund P., 2008. Holocene Glaciations in the Ema Glacier
700 Valley, Monte Sarmiento Massif, Tierra Del Fuego. Palaeogeography, Palaeoclimatology,
701 Palaeoecology 260, 299–314.
702
703 Strelin, J.A., Denton, G.H., Vandergoes, M.J., Ninnemann, U.S., Putnam, A.E., 2011. Radiocarbon
704 chronology of the late-glacial Puerto Bandera moraines, Southern Patagonian Icefield, Argentina.
705 Quaternary Science Reviews 30, 2551-2569.
706
707 Strelin, J., Kaplan, M., Vandergoes, M., Denton, G. & Schaefer, J., 2014. Holocene Glacier
708 Chronology of the Lago Argentino Basin, Southern Patagonian Icefield. Quaternary Science
709 Reviews 101, 124-145.
710
711 Stone, J. O., 2000. Air pressure and cosmogenic isotope production. Journal of Geophysical
712 Research 105, 23753-23759.
713
714 Stuiver, M., 1978. Radiocarbon timescale tested against magnetic and other dating methods
715 Nature 273, 271 – 274.
716
717 Villalba, R., Cook, E.R. D'Arrigo, R.D. Jacoby, G.C. Jones, P.D. Salinger, M.J., Palmer, J., 1997.
718 Sea-level pressure variability around Antarctica since A.D. 1750 inferred from subantarctic tree-
719 ring records. Climate Dynamics 13, 375-390.
720
721 Villalba, R., Masiokas, M., Kitzberger, T., Boninsegna, J.A., 2005. Biogeographical consequences
722 of recent climate changes in the southern Andes of Argentina. In Global Change and Mountain
723 Regions: An Overview of Current Knowledge. Series: Advances in Global Change Research, 23,
724 157-166.
725
726 Willis, M.J., Melkonian, A.K., Pritchard, M.E., Rivera, A., 2012. Ice loss from the Southern
727 Patagonian Ice Field, South America, between 2000 and 2012. Geophysical Research Letters 39,
728 10.1029/2012GL053136.

729
730 Xiao, W., Esper, O., Gersonde, R. 2016. Last Glacial - Holocene climate variability in the Atlantic
731 sector of the Southern Ocean 135, 115-137.
732
733 Yuan, X., Martinson, D.G., 2000. Antarctic Sea Ice Extent Variability and Its Global Connectivity.
734 Journal of Climate 13, 1697-1717.
735

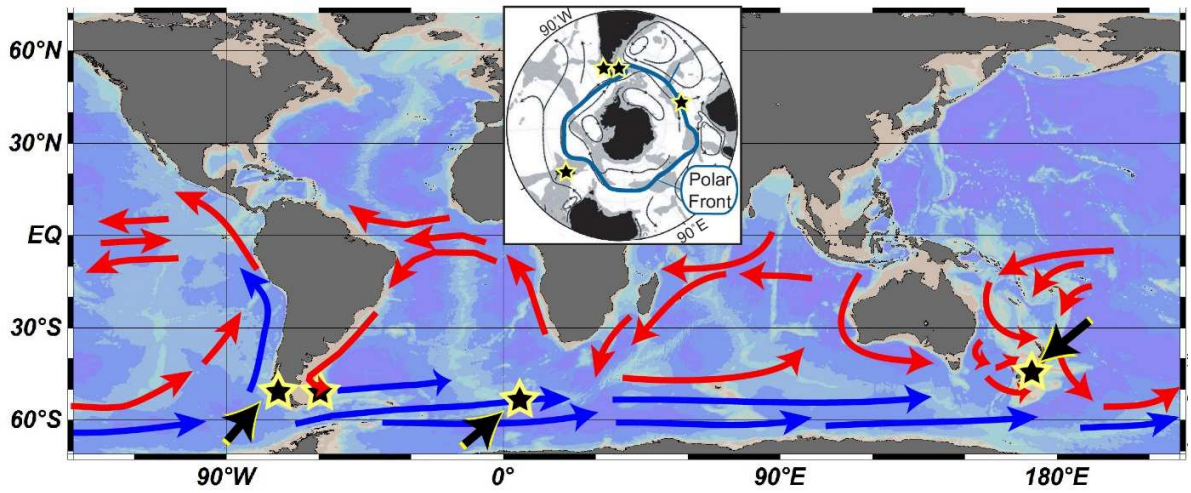

Figure 1. Setting of places discussed in the text (e.g., Figs. 2, 3, 6, 7), in a Southern Ocean and Polar context. Sites discussed (stars) include, from left to right, southern Patagonia (Fig. 2), Isla de los Estados (Fig. 7), TN057-13 (Figs. 6, 7) and South Island, New Zealand. For simplicity, currents are shown only for the Southern Hemisphere. Patagonia is downwind of the Southeast Pacific, where the cold Humboldt Current flows northward (Fig. 2). The location of TN057-13 is influenced by sub Antarctic climate regimes, being near the Polar front and northern limit of the sea ice influence (see text). Base image from Ocean Data View (ODV), http://odv.awi.de/.

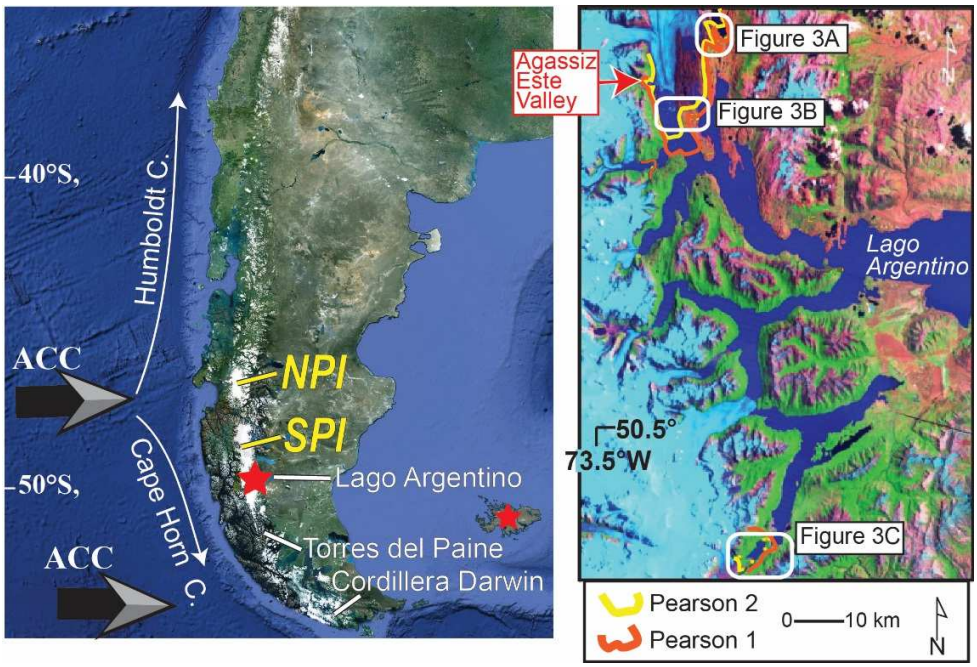

Figure 2. Setting of the Lago Argentino basin. Pearson 1 and 2 are two prominent landform complexes found throughout the basin, with the former occurring up to several kilometers beyond the latter (Mercer, 1968; Aniya, 1995; Aniya and Sato, 1995; Aniya et al., 1997; Malagnino and Strelin, 1992; Strelin et al., 2014). Evidence for the extent of glaciers during the early Holocene is best preserved in Agassiz Este Valley, near the present ice front (Fig. 5; Strelin et al., 2014). A star also marks Isla de los Estados (Fig. 7; Björck et al., 2012).

736

737

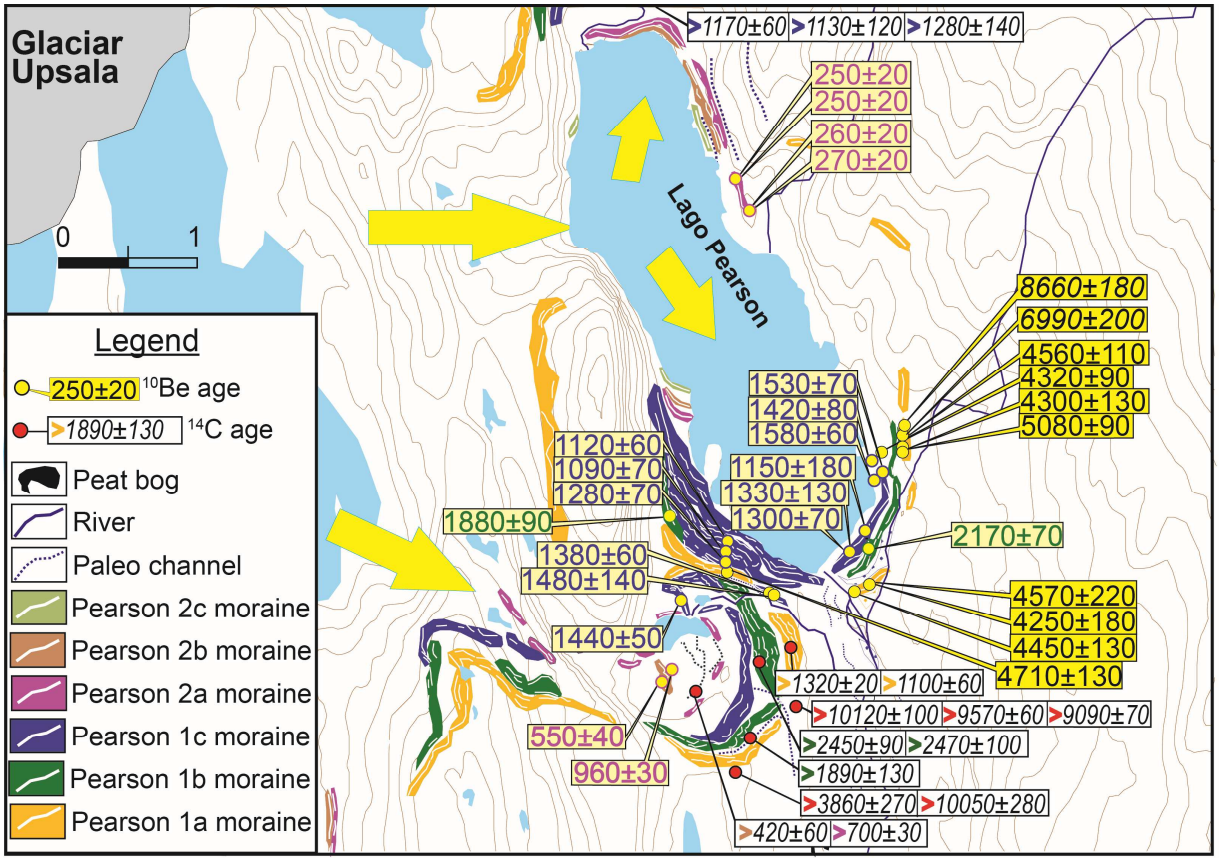

Figure 3A. Figures 3A to 3C cover three former outlet glaciers of the South Patagonian Icefield, Lago Pearson, Herminita-Brazo Upsala, and Lago Frías areas, respectively (Fig. 2). Geomorphic maps show landforms that represent former glacier margins (from Strelin et al., 2014). Also shown are ^{10}Be ages (±1σ analytical uncertainty) (Figs. 4-6, Tables S1 and 2), and ^{14}C ages (Fig. 5; Table S3, from Strelin et al., 2014). Colored symbols in front of ^{14}C ages correspond to moraine ages shown on Figure 5; if there is no symbol (Fig. 3B), then it dates the event. For more explanation of the ^{14}C data, see Table S3. Note that there was no lake (i.e., no calving) around Lago Pearson when the outer moraines formed. The legend applies to Figure 3A and B. Known outliers are in italics.

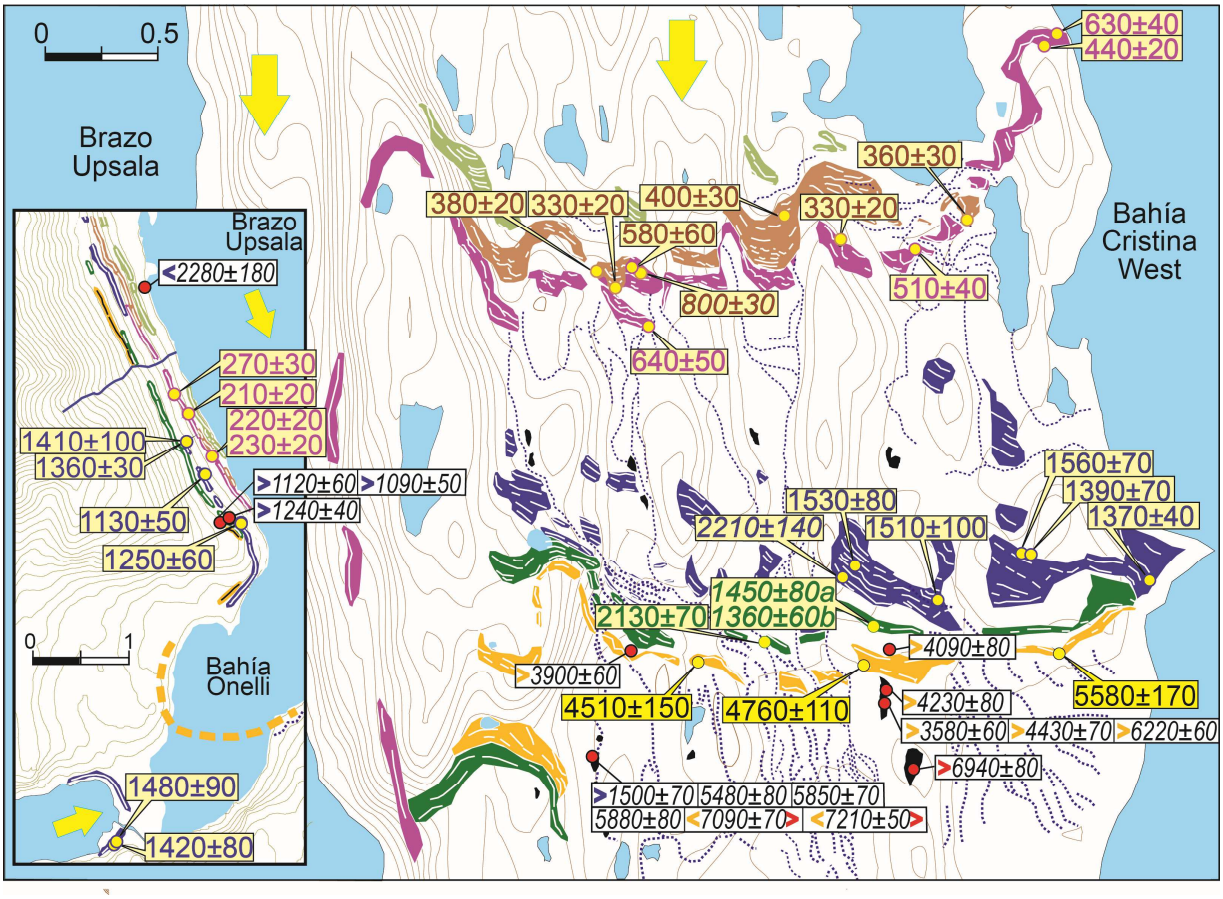

Figure 3B. The Herminita-Onelli area. The legend is the same as in Figure 3A.

738

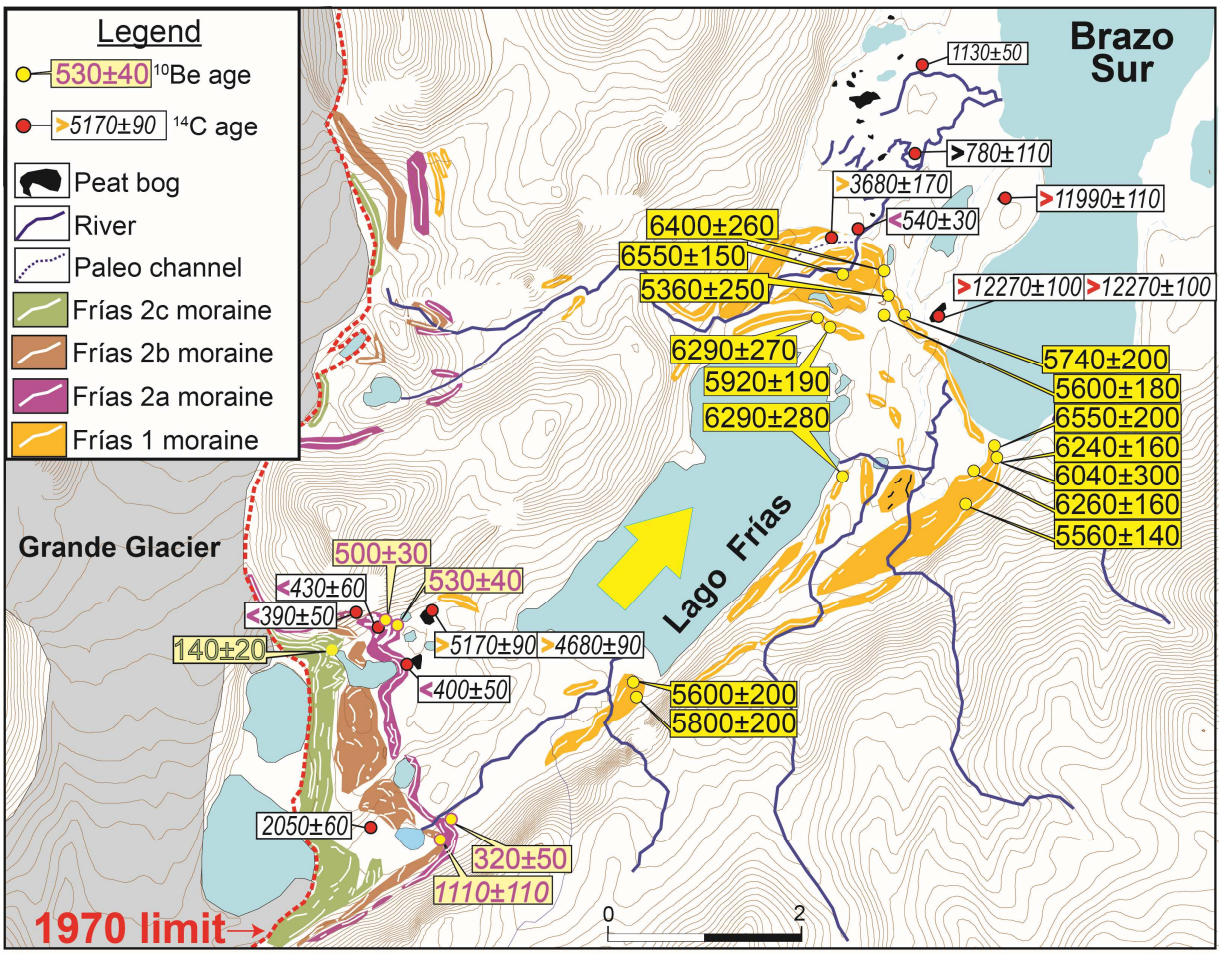

Figure 3C. The Lago Frías valley. Note that there was no lakes (i.e., no calving) when the moraines formed.

739

740

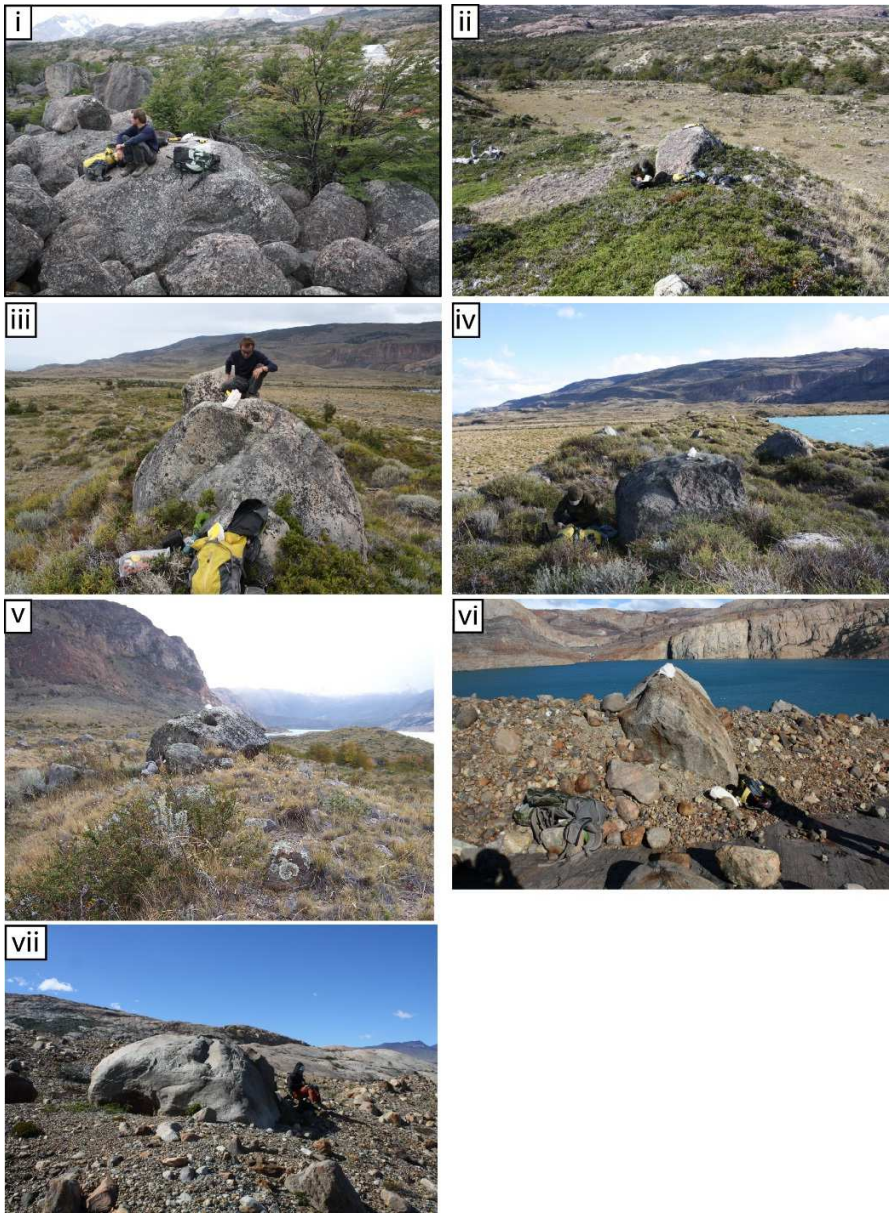

Figure 4A. Photographs of sampled boulders and moraines in the Lago Pearson area. **i)** Sample PE-10-02 (4,300±130) is on the top of a Pearson 1a left lateral crest. The photo is looking towards the northeast. Glacially-scoured terrain deglaciated in the early Holocene is seen beyond Pearson 1A. **ii)** PE-09-45 (4570±220) is rooted in the top of a Pearson 1a left lateral crest. The photo is looking towards the northeast. **iii)** PE-10-04 (2,170±70) is rooted in the top of a Pearson 1b left lateral crest. The photo is looking towards the south-southwest. **iv)** PE-09-48 (1,300±70) is rooted in the top of a Pearson 1c left lateral crest. The photo is looking towards the southwest. In the background of the photo are outwash (subaerial) deposits from the Lago Pearson lobe that surround the lake. **v)** PE-07-32 (1,120±60) is rooted in the top of a Pearson 1c right lateral crest in front of Lago Pearson. The photo is looking northward. Lago Pearson is in the background. **vi)** PE-10-07 (270±20) is rooted in a crest in front of Lago Pearson. The photo is looking towards the east. In the background is the Fossil Canyon, which was the source of outlet lobe that formed this moraine. Note freshness of the deposit and it overlies striated bedrock. **vii)** PE-10-09 (250±20) is in a crest in front of Lago Pearson. The photo is looking towards the west. Note the freshness of the deposit given it is ~240 years old (Fig. 3A).

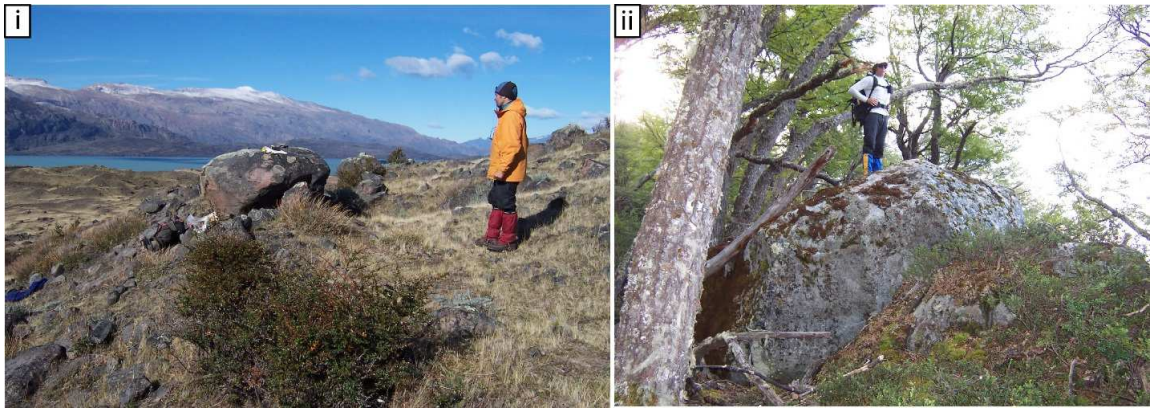

Figure 4B. Photographs of sampled boulders and moraines in the Herminita-Brazo Upsala area. **i)** Sample PE-06-08 (1,530±80) on the top of the fifth Pearson 1c crest. The photo is looking towards the southeast and other Pearson 1 ridges are seen in the background (from Strelin et al., 2014). **ii)** Sample PE-07-04 (230±20) is rooted in the top of a Pearson 1c right lateral crest adjacent to Bahía Upsala.

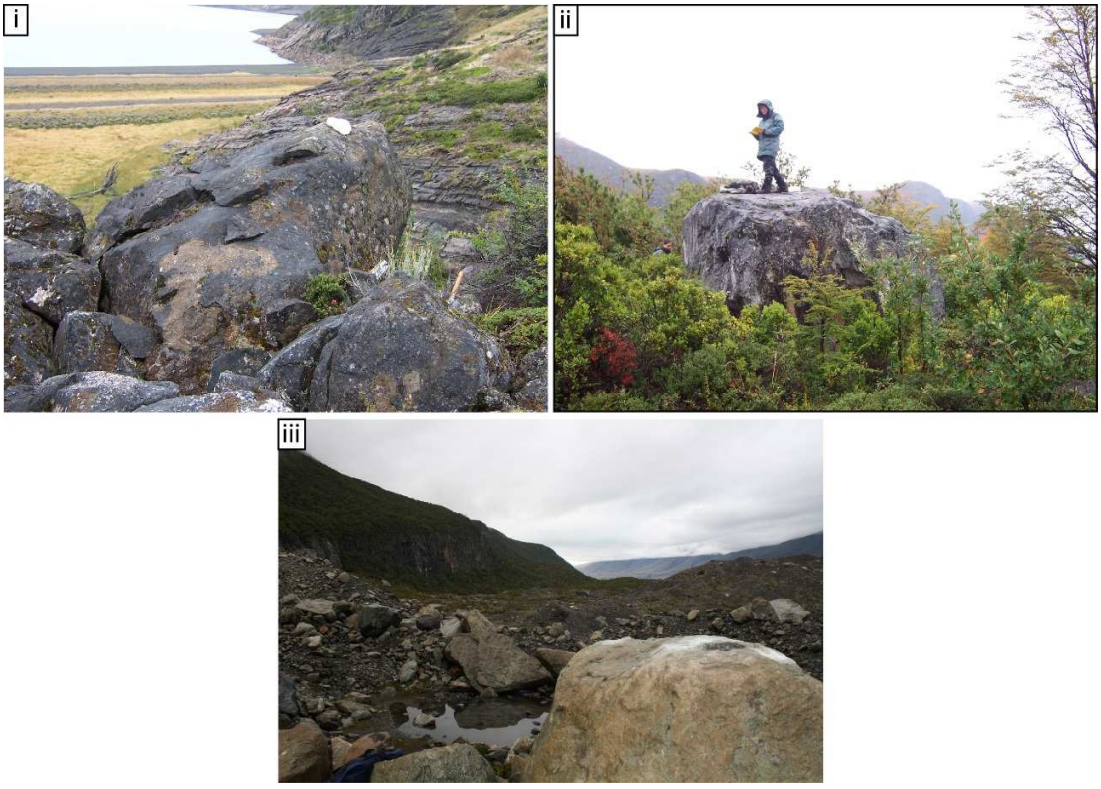

Figure 4C. Photographs of sampled boulders and moraines in the Frías Lobe, Figure 3C. **i)** Sample FR-07-02 (6,550±200) is on the top of a Frías 1 crest. The photo is looking towards the north and Brazo Sur is seen in the background. **ii)** Sample FR-07-14 (6,290±270) is on the top of a Frías 1 crest. The photo is looking towards the northwest. Note the top of the boulder is well above surrounding vegetation. **iii)** Sample FR-07-31 (140±20) is on the top of a Frías 2 crest. The whitish areas on top of the boulder are the sampled spots. The photo is looking towards the northeast and other Frías 2 ridges are seen in the background, including the area of samples FR-07-29 and -30.

741

742

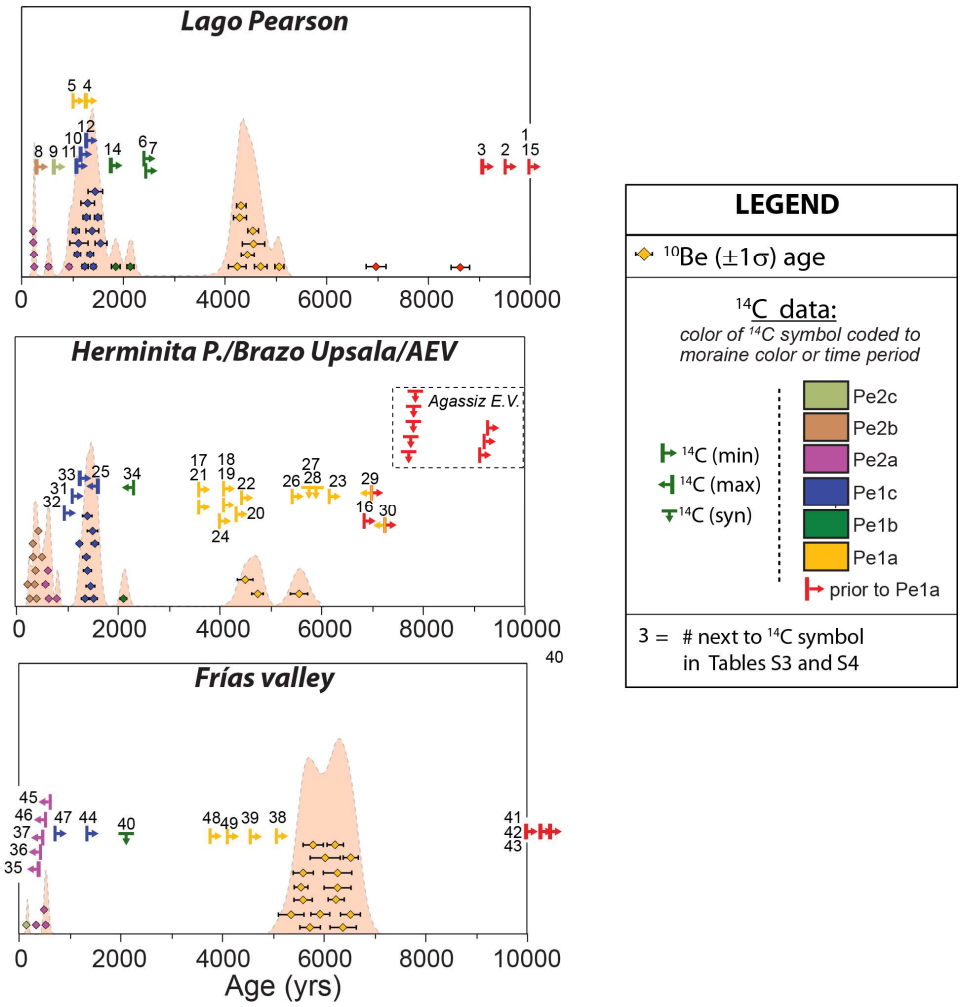

Figure 5. Plot of ^{10}Be and ^{14}C ages used to define glacial histories in the Lago Argentino basin. All ^{10}Be and ^{14}C ages are listed in Table S1 to S4. The number next to each symbol corresponds to the ^{14}C ages (shown on Fig. 3) in Tables S3 and S4. Moraine names follow Figure 3 and Strelin et al. (2014). Behind the ^{10}Be ages are summed probability distributions or 'camel humps' of all ages. On the Herminita Peninsula there are at least two Pearson 1a (Pe1a) moraines represented (Fig. 3B). Minimum-limiting ^{14}C ages older than 10 ka, which define the timing of deglaciation from Late Glacial limits (Strelin et al., 2011), are shown along the right border of the top and bottom panels. Ages from Agassiz Este Valley (AEV) are plotted in the middle panel; here, the ages >6 ka define glacial limits close to the present ice front (Strelin et al., 2014). This figure also highlights that ^{14}C ages often provide underestimated minimum or maximum-limiting ages and thus only bracket the timing of moraine building events.

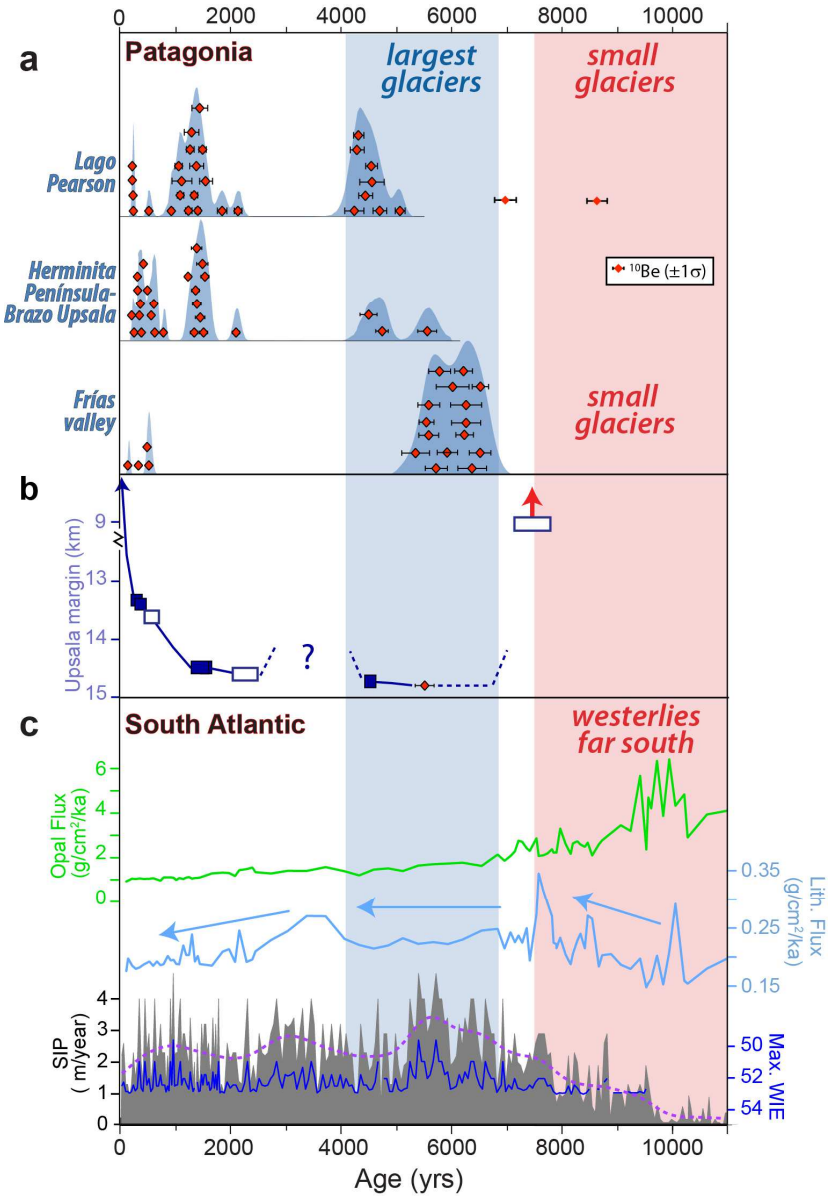

Figure 6. Southern South American and South Atlantic climate patterns. **a)** ^{10}Be and summed probability density plots of all the ages shown in Figure 3a-c.The 'camel humps' essentially reflect times of moraine formation. **b)** Time-distance plot for the Upsala ice front relative to modern, which incorporates data on Figures 3A and B and average moraine ages. Closed and open rectangles symbolize ^{10}Be- and ^{14}C-dated frontal limits, respectively. Also shown is an advance ^{14}C-dated to ~8-7 ka in Agassiz Este Valley (Fig. 2; Strelin et al., 2014). Not shown is the 6.1±0.4 ka advance of the Frías Glacier at the southernmost site (Fig. 3C). **c)** Opal and lithogenic flux data are from core TN057-13. Arrows in blue reflect overall net changes, as discussed in the text: WIE = winter ice edge latitude (dark blue); SIP= Sea ice presence (black); dashed purple line represents 1000-year smoothing.

743

744

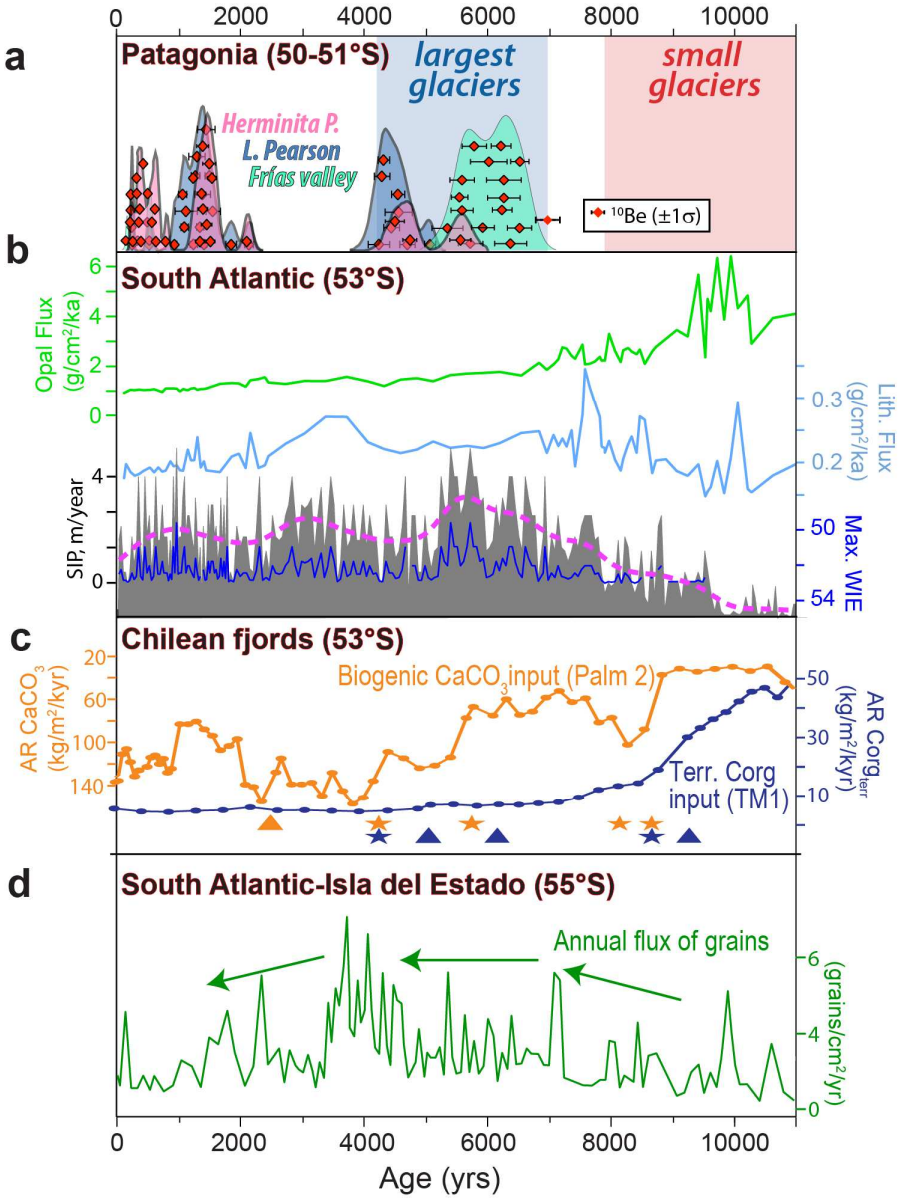

Figure 7. Comparison of records from near southern South America and in the South Atlantic. a) and b) are from Figure 6. **c)** Data are from Lamy et al. (2010). Biogenic $CaCO_3$ is inferred to be a proxy for salinity, which is a function of rainfall from the continent, with times of higher values reflecting the proximity of intense westerlies. Triangles indicate stratigraphic levels of ^{14}C ages and stars ash-layers. AR=accumulation rates; C_{org}=organic carbon. **d)** Data are from Björck et al. (2012). The annual flux of grains is inferred to be influenced by wind conditions.

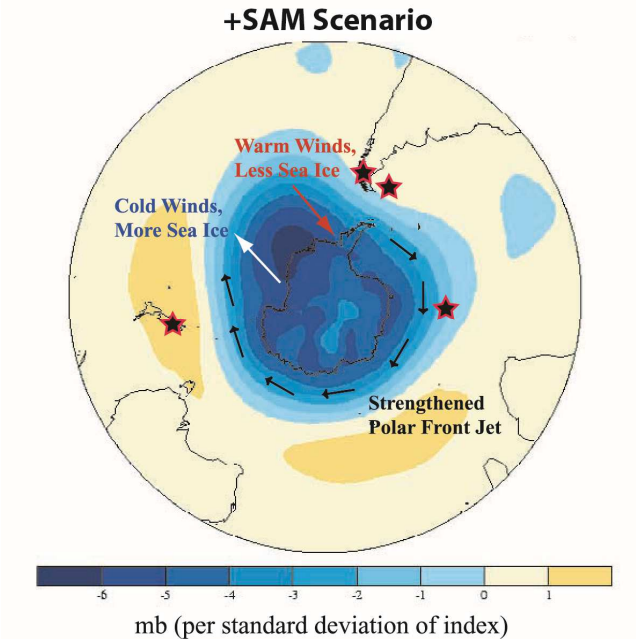

Figure 8. From Stammerjohn et al. (2008). Schematic depiction of high-latitude polar ice-atmosphere responses to a positive Southern Annular Mode (SAM). In the case shown, the "eccentricity" of the polar vortex (Pittock, 1980) is a function of the response to a positive SAM, with the arrows schematically depicting wind anomalies during such a scenario. We hypothesize that such a scenario may have been typically dominant during the early Holocene. Other discussions of the dynamics of the polar vortex and its consequential spatiotemporal effects on Southern Hemisphere climate are in Villalba et al. (1997, 2005) and Pittock (1980).

745